Object Classification using Electromagnetic Data and Neural Networks

Ergun Simsek
Dept. of Computer Science & Electrical Engineering
University of Maryland Baltimore County
Baltimore, MD, USA
simsek@umbc.edu

Raonaqul Islam
Dept. of Computer Science & Electrical Engineering
University of Maryland Baltimore County
Baltimore, MD, USA
raonaqi1@umbc.edu

***Abstract*—We created a scatterer database based on the modified MNIST data set. Using simple neural networks, we achieve a 90% accuracy in classifying objects. We investigated the accuracy as a function of antenna number and data set size. For large data sets, neural networks exhibit a higher accuracy compared to other traditional machine learning methods.**

***Index Terms*—machine learning, classification, electromagnetic.**

I. Introduction

Electromagnetic inversion [1]–[3] pertains to the process of deducing the properties or parameters of a medium (such as the distribution of electrical permittivity or conductivity) by analyzing measurements of electromagnetic fields scattered or transmitted through the medium, as illustrated in Fig. 1(a). The primary objective of electromagnetic inversion is to extrapolate the internal structure or composition of an object or material, relying on the analysis of its interaction with incident electromagnetic waves, as exemplified in Fig. 1(c) for the targets depicted in (b). This holds particular significance in fields such as geophysics, medical imaging, and non-destructive testing. Traditional methods encounter challenges such as nonlinearity, ill-posedness, and high computational costs. Recent advancements leverage machine learning to address these issues effectively. On the other hand, electromagnetic classification, as discussed in reference [4], involves the categorization or labeling of objects based on their interaction with electromagnetic waves. It represents a form of pattern recognition where the objective is to assign predefined classes or categories to objects by extracting features from their electromagnetic responses. Unlike inversion, which concentrates on recovering the properties of a medium, electromagnetic classification focuses on identifying or classifying objects themselves, as depicted in Fig. 1(d). This has diverse applications, including target recognition in radar systems, object identification using electromagnetic sensors, and material classification based on electromagnetic signatures. In contrast to conventional approaches often centered around signal processing, this research exclusively explores machine learning-based object classification utilizing electromagnetic data. While computer vision has achieved automated recognition, our work delves into the potential of classifying objects based on scattered electromagnetic waves, with implications for robotics and environmental perception.

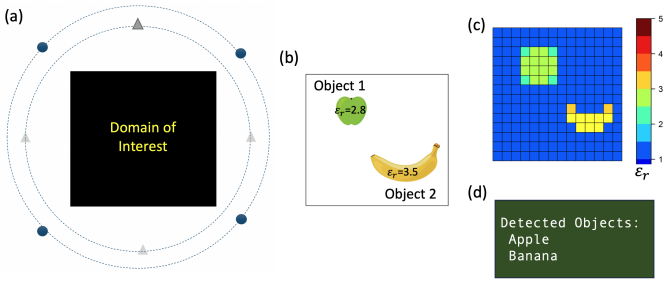

Fig. 1. (a) Schematic illustration of a measurement setup that is typically used in electromagnetic inversion. (b) Two objects are placed in the black box. (c) In electromagnetic inversion, the relative permittivity map is obtained with a CNN. (d) In electromagnetic classification, the output is simply the labels (classes) of the objects.

II. Data Set Preparation

The Modified National Institute of Standards and Technology (MNIST) dataset, extensively utilized in the fields of machine learning and computer vision, consists of grayscale images featuring handwritten digits, each associated with specific labels. The 60,000 images from the MNIST dataset undergo a transformation, evolving into a scatterer database. This conversion involves mapping pixel intensity values (ranging from 0 to 255) to corresponding relative electrical permittivity values (ranging from 1 to 4). The electromagnetic scattering dataset is then systematically generated using the freely accessible 2D electromagnetic finite difference frequency domain simulation tool known as Ceviche [5].

The computational domain, depicted in Fig. 2(a), is characterized by dimensions of $2\lambda \times 2\lambda$, featuring a uniform mesh along the x and y directions ($\Delta x = \Delta y = \lambda/150$), where λ denotes the wavelength of electromagnetic waves emitted by a transmitter antenna. Perfectly matched layers with a thickness of $\lambda/7.5$ are integrated into the setup. Initially, each cell's permittivity is assumed to be 1. Subsequently, a region measuring 140 pixels by 140 pixels at the center of the domain undergoes an update of permittivity using 2D cubic interpolation. The setup involves the placement of

978-1-7335096-7-1

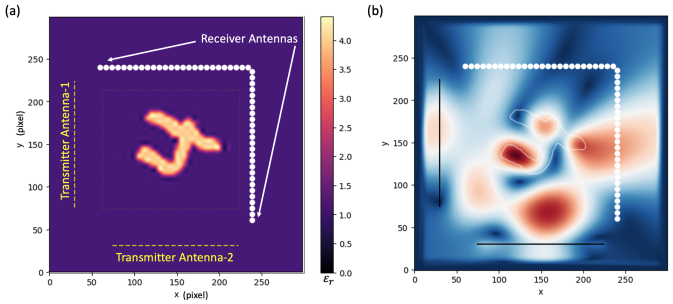

Fig. 2. (a) Permittivity distribution for one of the example geometries studied. The purple regions have a relative permittivity of 1. The regions with higher relative permittivity values are represented by lighter colors. The locations of transmitter antennas are indicated by yellow dashed lines, while white circles depict the positions of the 52 receiver antennas. (b) The solver calculates electric and magnetic fields all over the computation domain but we only use the data recorded at the receiver antennas.

two groups, each consisting of 26 receiver antennas, and two transmitter antennas at specific locations. Electromagnetic fields, exemplified in Fig. 2(b) for three field intensities, are computed at 52 receiver antennas for each transmitter antenna. This computation results in real and imaginary components stored in a dataset. The dataset's input section comprises 60,000 rows and 624 columns, representing receiver antennas, transmitter antennas, electromagnetic fields, and components. Meanwhile, the output section forms a $60,000 \times 1$ vector containing labels (digits).

III. Numerical Results

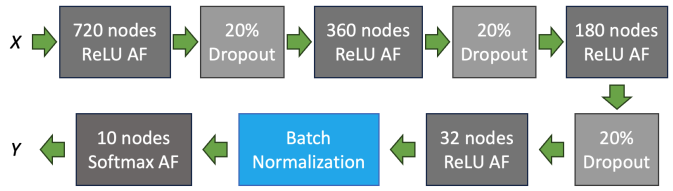

Fig. 3. Neural network architecture.

We utilize the functional application program interface (API) of Keras [6], running on top of TensorFlow [7]. The neural network architecture, illustrated in Figure 3, is composed of five hidden layers positioned between the input and output layers. The first four layers, containing decreasing number of neurons, are succeeded by dropout layers with a 20% dropout rate except the fourth one, which is followed with a batch normalization layer. The activation function for the initial four layers is the rectified linear unit (ReLU), while the last layer encompasses 10 nodes. The softmax activation function [9] is applied to this layer, generating probabilities for each label. For classification predictions, the class with the highest probability is selected. The learning rate is set to 10^{-3}, and the optimizer of choice is Adam [10]. Categorical cross-entropy [11] defines the loss function.

For the initial set of calculations, we allocate 50% of the dataset for training and the other 50% for testing, and we obtain an 90 % accuracy in classification as shown in Fig. 4 (a). The training takes approximately 21 minutes. To examine the impact of the training dataset size (N_{train}) on accuracy and training time, we conduct an additional set of calculations, varying N_{train} from 600 to 30,000. It is observed that the NN's accuracy increases with the the dataset size as expected. A training data set with 10000 samples guarantees a classification accuracy of 80%, while decreasing %25 reduction in the training time. At the conference, we provide more details on how accuracy changes with number of antennae.

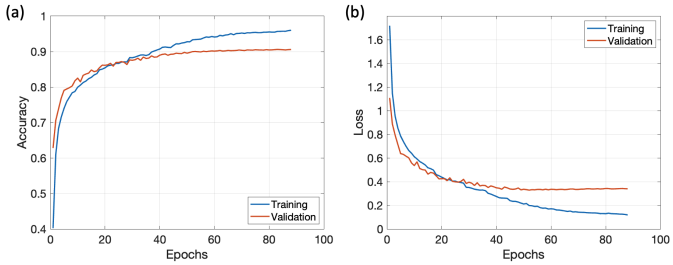

Fig. 4. (a) Accuracy and (b) loss vs. epochs.

IV. Conclusion

We have investigated the utilization of neural network methodologies within the domain of object classification using electromagnetic waves. Our findings indicate that it is viable to achieve a classification accuracy of 90% by training neural networks with the electromagnetic waves scattered from objects and corresponding labels.

References

[1] C. Y. Baojun Wei, Ergun Simsek and Q. H. Liu, "Three-dimensional electromagnetic nonlinear inversion in layered media by a hybrid diagonal tensor approximation: Stabilized biconjugate gradient fast fourier transform method," *Waves in Random and Complex Media*, vol. 17, no. 2, pp. 129–147, 2007.

[2] L. Li, L. G. Wang, F. L. Teixeira, C. Liu, A. Nehorai, and T. J. Cui, "Deepnis: Deep neural network for nonlinear electromagnetic inverse scattering," *IEEE Transactions on Antennas and Propagation*, vol. 67, no. 3, pp. 1819–1825, 2019.

[3] K. Xu, L. Wu, X. Ye, and X. Chen, "Deep learning-based inversion methods for solving inverse scattering problems with phaseless data," *IEEE Transactions on Antennas and Propagation*, vol. 68, no. 11, pp. 7457–7470, 2020.

[4] E. Simsek, "Classification with electromagnetic waves," *submitted to IEEE Transactions on Antennas and Propagation*, 2024.

[5] T. W. Hughes, I. A. Williamson, M. Minkov, and S. Fan, "Forward-mode differentiation of maxwell's equations," *ACS Photonics*, vol. 6, no. 11, pp. 3010–3016, 2019.

[6] F. Chollet *et al.*, "Keras," https://keras.io, 2015.

[7] A. Martin *et al.*, "TensorFlow: Large-scale machine learning on heterogeneous systems," 2015, software available from tensorflow.org. [Online]. Available: https://www.tensorflow.org/

[8] D. E. Rumelhart and J. L. McClelland, *Learning Internal Representations by Error Propagation*, 1987, pp. 318–362.

[9] P. Brown, J. Cocke, S. Della Pietra, V. Della Pietra, F. Jelinek, R. Mercer, and P. Roossin, "A statistical approach to language translation," in *Coling Budapest 1988 Volume 1: International Conference on Computational Linguistics*, 1988.

[10] D. P. Kingma and J. Ba, "Adam: A method for stochastic optimization," 2014.

[11] G. Tsoumakas and I. Katakis, "Multi-label classification: An overview," *International Journal of Data Warehousing and Mining (IJDWM)*, vol. 3, no. 3, pp. 1–13, 2007.